



**CHALMERS**  
UNIVERSITY OF TECHNOLOGY

## **10.13% Efficiency All-Polymer Solar Cells Enabled by Improving the Optical Absorption of Polymer Acceptors**

Downloaded from: <https://research.chalmers.se>, 2022-08-27 21:34 UTC

Citation for the original published paper (version of record):

Fan, Q., Ma, R., Liu, T. et al (2020). 10.13% Efficiency All-Polymer Solar Cells Enabled by Improving the Optical Absorption of Polymer Acceptors. Solar RRL, 4(6). <http://dx.doi.org/10.1002/solr.202000142>

N.B. When citing this work, cite the original published paper.

# 10.13% Efficiency All-Polymer Solar Cells Enabled by Improving the Optical Absorption of Polymer Acceptors

Qunping Fan, Ruijie Ma, Tao Liu,\* Wenyan Su, Wenhong Peng, Ming Zhang, Zaiyu Wang, Xin Wen, Zhiyuan Cong, Zhenghui Luo, Lintao Hou, Feng Liu, Weiguo Zhu,\* Donghong Yu, He Yan,\* and Ergang Wang\*

The limited light absorption capacity for most polymer acceptors hinders the improvement of the power conversion efficiency (PCE) of all-polymer solar cells (all-PSCs). Herein, by simultaneously increasing the conjugation of the acceptor unit and enhancing the electron-donating ability of the donor unit, a novel narrow-bandgap polymer acceptor PF3-DTCO based on an A–D–A-structured acceptor unit ITIC16 and a carbon–oxygen (C–O)-bridged donor unit DTCO is developed. The extended conjugation of the acceptor units from IDIC16 to ITIC16 results in a red-shifted absorption spectrum and improved absorption coefficient without significant reduction of the lowest unoccupied molecular orbital energy level. Moreover, in addition to further broadening the absorption spectrum by the enhanced intramolecular charge transfer effect, the introduction of C–O bridges into the donor unit improves the absorption coefficient and electron mobility, as well as optimizes the morphology and molecular order of active layers. As a result, the PF3-DTCO achieves a higher PCE of 10.13% with a higher short-circuit current density ( $J_{sc}$ ) of  $15.75 \text{ mA cm}^{-2}$  in all-PSCs compared with its original polymer acceptor PF2-DTC (PCE = 8.95% and  $J_{sc} = 13.82 \text{ mA cm}^{-2}$ ). Herein, a promising method is provided to construct high-performance polymer acceptors with excellent optical absorption for efficient all-PSCs.


state-of-the-art PSCs have achieved power conversion efficiencies (PCEs) of 16–18%.<sup>[5–17]</sup> Regarding such SM acceptor-based PSCs, the all-polymer solar cells (all-PSCs) consisting of a polymer donor and a polymer acceptor show unique advantages in the flexible large-scale and wearable energy generators due to their excellent morphology stability and mechanical robustness.<sup>[18–21]</sup> However, most of the efficient all-PSCs have PCEs ranging in 8–10%,<sup>[22–34]</sup> although a few of them achieved PCEs over 11%,<sup>[35–37]</sup> which is still far behind that of the efficient PSCs based on SM acceptors due to the lack of high-performance polymer acceptors. To date, polymer acceptors have been mainly confined into a small number of structural building blocks,<sup>[24–26,38–40]</sup> and the most widely studied one is the polymer N2200 with a donor–acceptor (D–A) backbone of naphthalene diimide (NDI)-*alt*-bithiophene due to its NBG and suitable molecular energy levels.<sup>[39–43]</sup> However, N2200 neat film suffers from a low absorption coefficient of  $\approx 0.3 \times 10^5 \text{ cm}^{-1}$  and an excess strong crystallinity and stacking, which usually lead to the limited photocurrent and large phase separation in active layers.<sup>[39–43]</sup>

During the past five years, polymer solar cells (PSCs) based on narrow bandgap (NBG) fused-ring small molecule (SM) acceptors have made considerable progress,<sup>[1–4]</sup> among which the

coefficient of  $\approx 0.3 \times 10^5 \text{ cm}^{-1}$  and an excess strong crystallinity and stacking, which usually lead to the limited photocurrent and large phase separation in active layers.<sup>[39–43]</sup>

Dr. Q. Fan, Dr. W. Su, W. Peng, X. Wen, Dr. Z. Cong, Prof. E. Wang  
Department of Chemistry and Chemical Engineering  
Chalmers University of Technology  
Göteborg SE-412 96, Sweden  
E-mail: ergang@chalmers.se

R. Ma, Dr. T. Liu, Dr. Z. Luo, Prof. H. Yan  
Department of Chemistry and Hong Kong Branch of Chinese National  
Engineering Research Center for Tissue Restoration & Reconstruction  
Hong Kong University of Science and Technology  
Clear Water Bay, Kowloon 999077, Hong Kong  
E-mail: liutaozhx@ust.hk; hyan@ust.hk

 The ORCID identification number(s) for the author(s) of this article can be found under <https://doi.org/10.1002/solr.202000142>.

© 2020 The Authors. Published by WILEY-VCH Verlag GmbH & Co. KGaA, Weinheim. This is an open access article under the terms of the Creative Commons Attribution License, which permits use, distribution and reproduction in any medium, provided the original work is properly cited.

DOI: 10.1002/solr.202000142

Dr. W. Su, Prof. L. Hou  
Guangdong Provincial Key Laboratory of Optical Fiber Sensing and  
Communications  
Guangzhou Key Laboratory of Vacuum Coating Technologies and New  
Energy Materials  
Siyuan Laboratory  
Department of Physics  
Jinan University  
Guangzhou 510632, P. R. China

W. Peng, Prof. W. Zhu  
School of Materials Science and Engineering  
Jiangsu Key Laboratory of Environmentally Friendly Polymeric Materials  
Jiangsu Engineering Laboratory of Light-Electricity-Heat Energy-Converting  
Materials and Applications  
Changzhou University  
Changzhou 213164, China  
E-mail: zwg@cczu.edu.cn, zhuwg18@126.com

Recently, a  $\pi$ -fused A–D–A-type building block IDIC16 was introduced as an acceptor unit to develop a promising high-performance alternative polymer acceptor PZ1 with thiophene as a donor unit, which shows a comparable NBG and a high absorption coefficient ( $>10^5 \text{ cm}^{-1}$ ) and thus an impressive PCE of 9.19% with a high  $J_{sc}$  over  $16 \text{ mA cm}^{-2}$  in its all-PSCs.<sup>[25]</sup> Subsequently, by changing the donor unit from thiophene to benzodithiophene, an IDIC16-based polymer acceptor PFBTD-IDTIC was synthesized, leading to an improved PCE over 10% in its all-PSCs.<sup>[23]</sup> Moreover, another polymer acceptor PN1 was developed by modifying the acceptor unit from IDIC16 to MOITIC16 with a larger  $\pi$ -fused structure and a bulky sterically hindered phenyl side chain and also an increased PCE over 10% in its all-PSCs was obtained.<sup>[44]</sup> Compared with the original polymer PZ1, the aforementioned polymer acceptors were developed by either optimizing the donor unit or acceptor unit, showing a blue-shifted absorption spectrum or a decreased absorption coefficient, which results in a smaller  $J_{sc}$  of  $\approx 15 \text{ mA cm}^{-2}$  and thus limits further improvement of PCE in all-PSCs.<sup>[23,44]</sup> Recently, our work shows that the bridging atoms in the donor unit can significantly influence the absorption coefficient and crystallinity of polymer acceptors, as well as the morphology and molecular order of the active layer blends.<sup>[45]</sup> Therefore, an efficient strategy to construct polymer acceptors with excellent optical absorption capacity and suitable crystallinity will be conducted to further improve device efficiencies.

Herein, a series of D–A polymer acceptors PF2-DTC, PF3-DTC, and PF3-DTCO with NBG were developed by increasing the conjugated length of the acceptor unit from *s*-indacenodithiophene-based IDIC16 to dithieno-*s*-indacenodithiophene-based ITIC16 and enhancing the electron-donating ability of the donor unit from carbon (C)-bridged DTC unit to carbon–oxygen (C–O)-bridged DTCO unit in turn (Scheme 1a). Compared with the original PF2-DTC, PF3-DTC shows a broadened absorption spectrum and a higher absorption coefficient with an almost unchanged lowest unoccupied molecular orbital (LUMO) level. Moreover, in addition to further broadening the absorption spectrum via the enhanced intramolecular charge transfer (ICT) effect, the introduction of C–O bridges into donor unit also improves the absorption coefficient and electron mobility, as well as the morphology and molecular order of the active layer blends. As a result, PF3-DTCO achieved the highest PCE of 10.13% with a significantly improved  $J_{sc}$  of  $15.75 \text{ mA cm}^{-2}$  and a fill factor (FF) of 68.2% in all-PSCs compared with those of PF2-DTC (PCE = 8.95%) and PF3-DTC (PCE = 7.83%). Our

work not only developed a high-performance polymer acceptor, but also demonstrated a promising method to construct efficient D–A polymer acceptors by synergistically optimizing the acceptor and donor units for efficient all-PSCs.

The monomer ITIC16-Br was synthesized via Knoevenagel condensation, as shown in Scheme 1b, and the corresponding <sup>1</sup>H NMR spectrum is shown in Figure S1, Supporting Information. Then, the IDIC16-based polymer PF2-DTC and ITIC16-based polymers PF3-DTC and PF3-DTCO were obtained via Stille-coupling polymerization. Thanks to the long and multiple-solubilizing alkyl side chains in both donor and acceptor units, these three polymers exhibit reasonably high molecular weights with number average molecular weights of 23.8, 22.3, and 11.9 kDa and polydispersity indexes of 3.92, 2.33, and 3.21, respectively, but still good solubility in common organic solvents (such as chloroform and chlorobenzene).

As shown in Figure 1a and Figure S2, Supporting Information, of UV–vis measurements, these polymer acceptors show gradually red-shifted absorption spectra and increased absorption coefficients from the original PF2-DTC to PF3-DTC and then to PF3-DTCO due to the increased conjugation length of acceptor units from IDIC16 to ITIC16, as well as the increased ICT effect, resulting from the improved electron-donating ability of donor units from DTC to DTCO in turn. As a result, PF3-DTCO film shows the smallest bandgap of 1.50 eV with an absorption onset of  $\approx 825 \text{ nm}$  and the highest absorption coefficient of  $1.34 \times 10^5 \text{ cm}^{-1}$  at 745 nm, which is much better than the original PF2-DTC with a bandgap of 1.58 eV, an absorption onset of 785 nm, and an absorption coefficient of  $1.24 \times 10^5 \text{ cm}^{-1}$  at 720 nm. Figure 1b shows the molecular energy levels of photovoltaic materials, and the corresponding cyclic voltammograms are shown in Figure S3, Supporting Information. In accordance with the UV–vis results with the decreased optical bandgap in turn, these polymer acceptors display the gradually decreased electrochemical bandgap from PF2-DTC to PF3-DTC and then to PF3-DTCO, in which the related LUMO down-shifted and HOMO up-shifted gradually.

As shown in Figure 1c–e and Figure S4, Supporting Information, from grazing incidence wide-angle X-ray scattering (GIWAXS) measurements,<sup>[46]</sup> the three polymer acceptor films do not have obvious lamellar (100) diffraction peak in-plane (IP) profiles, whereas the PF3-DTCO film has a weak (100) diffraction peak in  $0.266 \text{ \AA}^{-1}$ . The strong  $\pi$ – $\pi$  stacking (010) diffraction peaks with the crystallite coherence lengths (CCLs) of 11.51–13.25  $\text{\AA}$  at out-of-plane (OOP) profiles were observed,

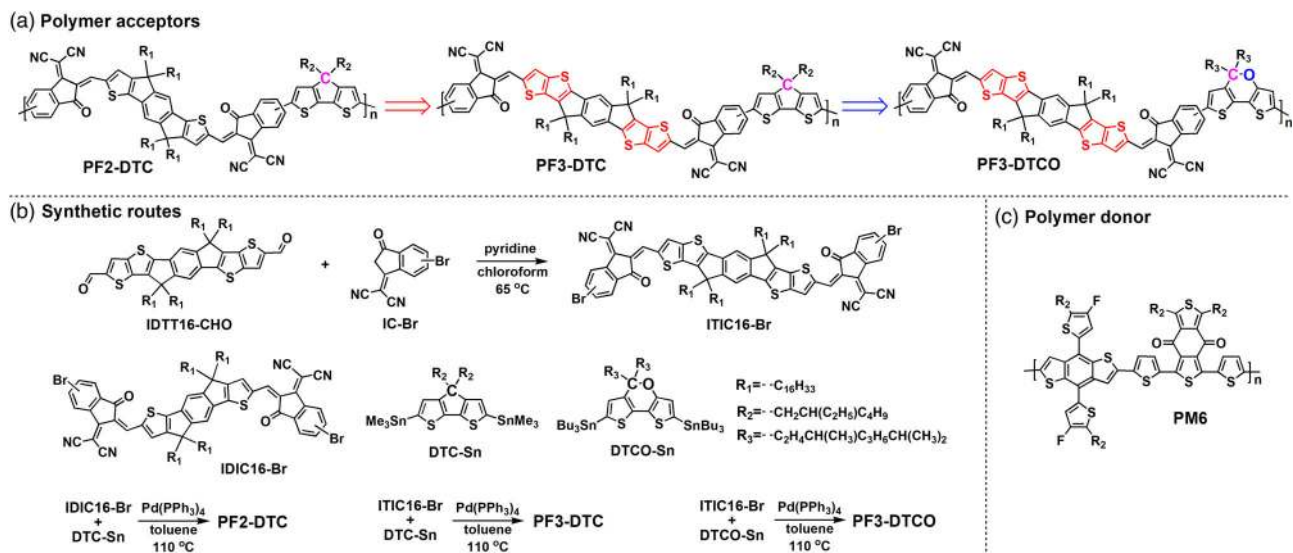
M. Zhang, Z. Wang, Prof. F. Liu  
Department of Physics and Astronomy  
Shanghai Jiaotong University  
Shanghai 200240, China

Dr. Z. Cong  
State Key Laboratory of Fluorine & Nitrogen Chemicals  
Xi'an Modern Chemistry Research Institute  
Xi'an 710065, China

Prof. D. Yu  
Department of Chemistry and Bioscience  
Aalborg University  
Aalborg DK-9220, Denmark

Prof. D. Yu  
Sino-Danish Center for Education and Research  
Aarhus DK-8000, Denmark

Prof. E. Wang  
School of Materials Science and Engineering  
Zhengzhou University  
Zhengzhou 450001, China



**Scheme 1.** a) Molecular structures of three polymer acceptors PF2-DTC, PF3-DTC, and PF3-DTCO. b) Synthetic routes of three polymer acceptors. c) Molecular structure of polymer donor PM6.

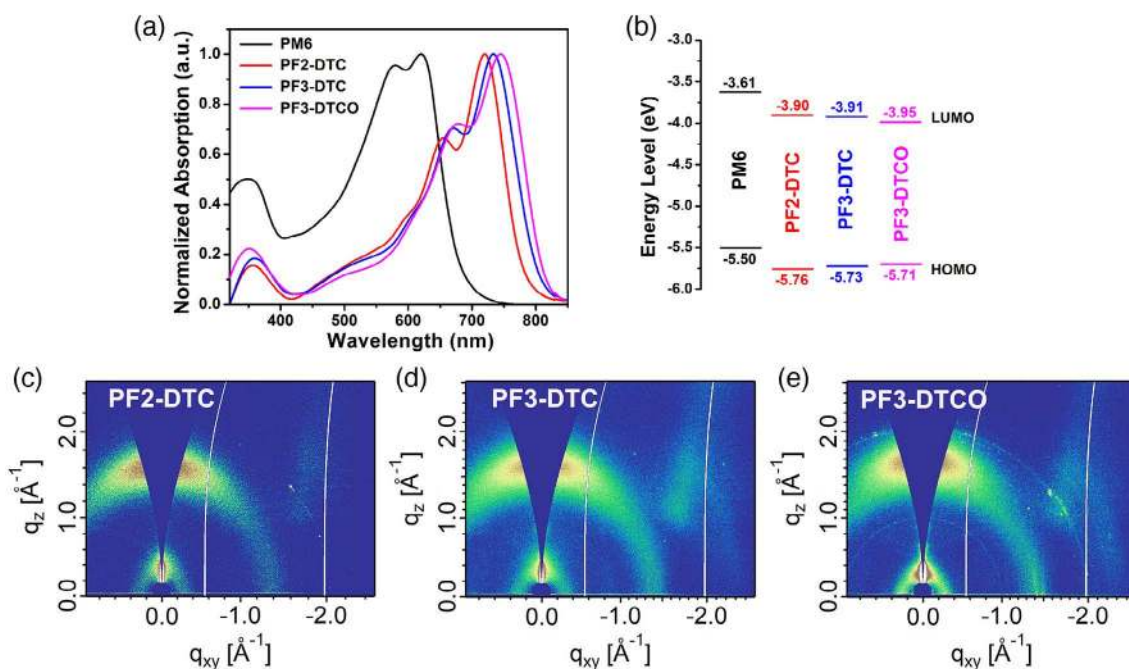


**Figure 1.** a) Normalized absorption spectra and b) energy-level diagrams of active layer materials in neat films. c) 2D GIWAXS images of three polymer acceptors.

indicating the predominant “face-on” orientation for these three polymer acceptor films. From PF2-DTC to PF3-DTC and then to PF3-DTCO, these neat films show gradually decreased  $\pi$ - $\pi$  stacking spacing from 3.99 to 3.94 and then to 3.84 Å. As shown in Figure S5, Supporting Information, estimated by the space charge limited current (SCLC) method, PF3-DTCO shows the highest electron mobility ( $\mu_e$ ) of  $8.32 \times 10^{-4} \text{ cm}^2 \text{ V}^{-1} \text{ s}^{-1}$  compared with those of PF2-DTC ( $7.13 \times 10^{-4} \text{ cm}^2 \text{ V}^{-1} \text{ s}^{-1}$ ) and PF3-DTC ( $7.23 \times 10^{-4} \text{ cm}^2 \text{ V}^{-1} \text{ s}^{-1}$ ).

The all-PSCs with a device structure of ITO/PEDOT:PSS/PM6:acceptor/PNDIT-F3N/Ag were fabricated to probe the photovoltaic performance of polymer acceptors. As the three polymer acceptors have similar molecular structures, the same optimized procedures were applied for all these all-PSCs, in which the thickness of the spin-coated active layer is  $\approx 100 \text{ nm}$  from a blend solution of chloroform:1-chloronaphthalene (CF:CN, 100:4 in v/v) with a total solid concentration of  $8 \text{ mg mL}^{-1}$  and a D/A ratio (w/w) of 2:1. As shown in Figure 2a

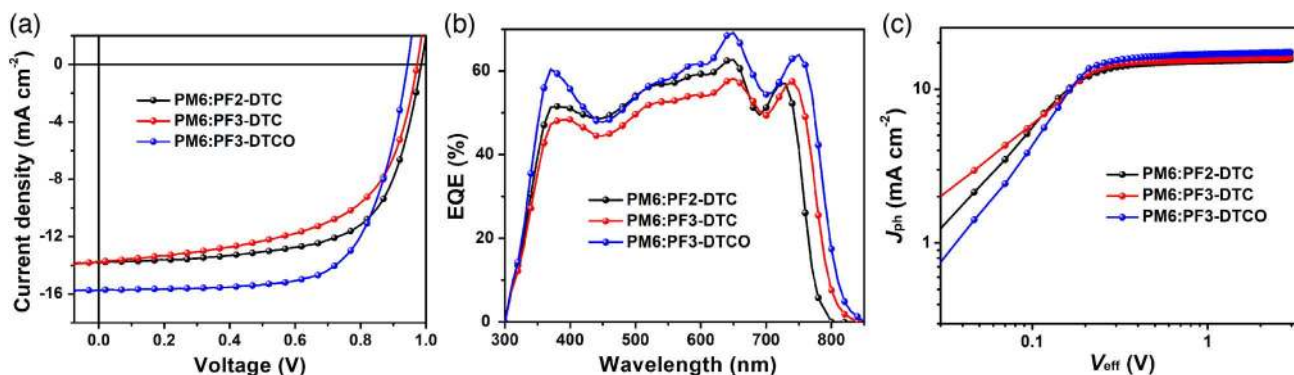


**Figure 2.** a) The  $J$ - $V$  plots of the optimized all-PSCs based on three different polymer acceptors under the illumination of AM 1.5G,  $100 \text{ mW cm}^{-2}$ . b) The corresponding EQE spectra and c) the  $J_{ph}$  versus  $V_{eff}$  curves of the three optimized all-PSCs.

of the current density–voltage ( $J$ - $V$ ) curves, from PF2-DTC to PF3-DTC and then to PF3-DTCO, the related all-PSCs show a gradually decreased  $V_{oc}$  from 0.986 to 0.943 V, which is consistent with their down-shifted LUMO levels. Compared with the PF2-DTC-based device, the PF3-DTC-based device shows a similar  $J_{sc}$  of  $\approx 13.8 \text{ mA cm}^{-2}$  but a significantly decreased FF from 65.7% to 58.5%, which may be due to the strong self-aggregation of PF3-DTC in the blend film, leading to excessive phase separation (see **Figure 3**). Notably, the PM6:PF3-DTCO-based all-PSCs obtained the highest PCE of 10.13% with an obviously higher  $J_{sc}$  of  $15.75 \text{ mA cm}^{-2}$  and FF of 68.2% compared with those of the all-PSCs based on PM6:PF2-DTC (PCE = 8.95%) and PM6:PF3-DTC (PCE = 7.83%).

The external quantum efficiency (EQE) measurements were carried out to verify the accuracy of the photovoltaic performance of all-PSCs. As shown in **Figure 2b**, the all-PSCs based on different polymer acceptors from PF2-DTC to PF3-DTC and then to PF3-DTCO show gradually red-shifted EQE spectra, which is consistent with the UV-vis spectra of their blend films (**Figure S6**, Supporting Information). Compared with the PF2-DTC-based device, the PF3-DTC-based one shows lower EQE response values, which could be due to the excessive phase separation of the active layer materials (**Figure 3**), resulting in weak exciton dissociation probability  $P(E,T)$  (see **Figure 2c**). Among these all-PSCs, the PF3-DTCO-based device has the higher EQE values in almost the entire spectral range, the

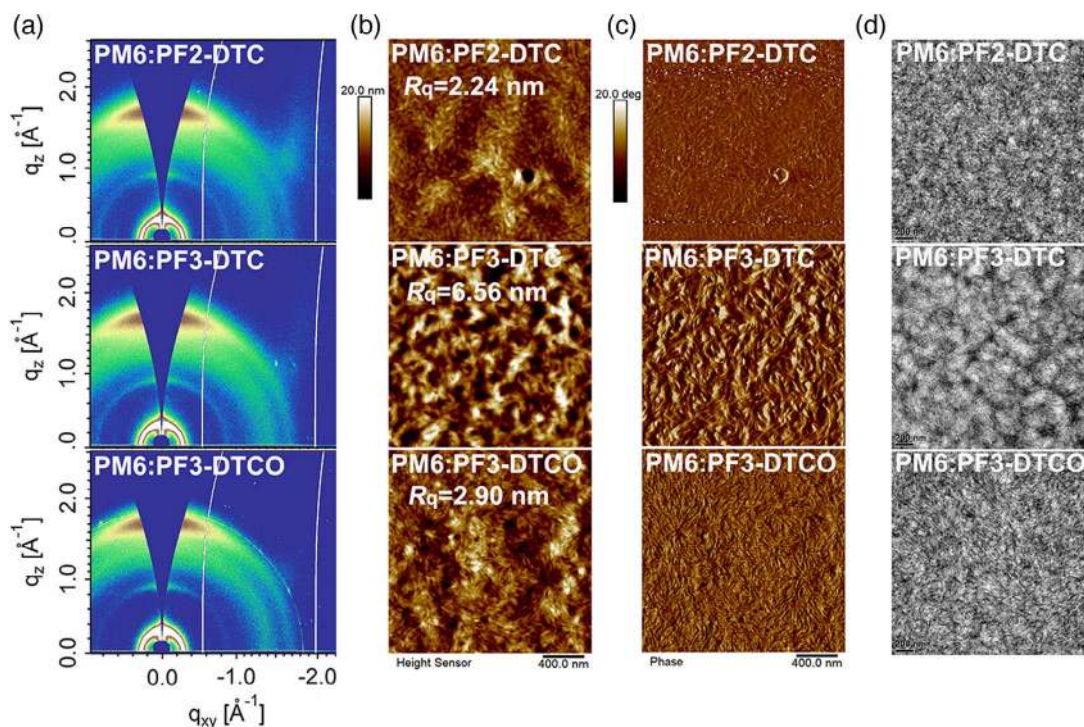


**Figure 3.** a) The 2D GIWAXS profiles, b) the AFM height images, c) the AFM phase images, and d) the TEM images of all-polymer blend films, respectively.

**Table 1.** Photovoltaic data of the three optimized all-PSCs.

Active layer	$V_{oc}$ [V]	$J_{sc}$ [ $\text{mA cm}^{-2}$ ] <sup>a)</sup>	FF [%]	PCE [%] <sup>b)</sup>	$P(E, T)$ [%]
PM6:PF2-DTC	0.986	13.82 (13.49)	65.7	8.95 (8.76)	71.5
PM6:PF3-DTC	0.973	13.77 (13.42)	58.5	7.83 (7.83)	61.5
PM6:PF3-DTCO	0.943	15.75 (15.48)	68.2	10.13 (9.84)	77.7

<sup>a)</sup>The integral  $J_{sc}$  in parenthesis from the EQE curves; <sup>b)</sup>The average PCEs in parenthesis calculated from 20 different devices.

corresponding highest EQE value is close to 70%. As shown in **Table 1**, the mismatch between the integrated  $J_{sc}$  from EQEs and the measured  $J_{sc}$  from  $J$ - $V$  plots is only  $\approx 2\%$ , suggesting the high reliability of the photovoltaic performance data in this work.

To understand why the PF3-DTCO-based device has the highest  $J_{sc}$  and FF values among three types of devices, their  $P(E, T)$ <sup>[47]</sup> estimated by the plots of photocurrent ( $J_{ph}$ ) versus effective voltage ( $V_{eff}$ ) and charge mobilities estimated by the SCLC method were studied. As shown in Figure 2c and Table 1, compared with the PF2-DTC-based device with a  $P(E, T)$  of 71.5%, under the maximal power output condition, the PF3-DTC-based one shows a significantly lower  $P(E, T)$  of 61.0%, whereas the PF3-DTCO-based device has a higher  $P(E, T)$  of 77.7%. As shown in Figure S7, Supporting Information, compared with the PF2-DTC-based device with the hole and electron mobilities ( $\mu_h$  and  $\mu_e$ ) of  $6.31 \times 10^{-4}$  and  $3.41 \times 10^{-4} \text{ cm}^2 \text{ V}^{-1} \text{ s}^{-1}$  and the PF3-DTC-based device with the  $\mu_h$  and  $\mu_e$  of  $6.18 \times 10^{-4}$  and  $2.88 \times 10^{-4} \text{ cm}^2 \text{ V}^{-1} \text{ s}^{-1}$ , the PF3-DTCO-based device shows the similar but slightly higher  $\mu_h$  and  $\mu_e$  of  $7.18 \times 10^{-4}$  and  $4.21 \times 10^{-4} \text{ cm}^2 \text{ V}^{-1} \text{ s}^{-1}$  with a smaller  $\mu_h/\mu_e$  ratio. The higher  $P(E, T)$  and the increased  $\mu_h$  and  $\mu_e$  with a more balanced  $\mu_h/\mu_e$  are conducive for optimizing the exciton dissociation and charge extraction, as well as suppressing the accumulation of space charge in devices.

The GIWAXS, atomic force microscopy (AFM), and transmission electron microscopy (TEM) measurements were carried out to probe the molecular crystallinity and packing, as well as surface and bulk separation morphologies of the blend films. Figure 3a and Figure S8, Supporting Information, summarize the 2D GIWAXS diffraction images and the related OOP and IP line cuts of the blend films. All the blend films display a predominant orientation of “face on.” Upon mixing with the polymer donor PM6, the blend films show significantly enhanced (100) diffraction peaks with much higher CCLs of 169.9–177.5 Å in the IP direction compared with the PM6 neat film (see Figure S9, Supporting Information) with a CCL of 57.0 Å. In the OOP direction, the PM6:PF2-DTC and PM6:PF3-DTC blend films show similar  $\pi$ - $\pi$  stacking with distance of 3.70 Å, whereas the PM6:PF3-DTCO blend film shows a slightly smaller  $\pi$ - $\pi$  stacking spacing of 3.68 Å, which is consistent with the trend observed in neat films. As shown in Figure 3b,c, compared with the PF2-DTC-based blend with a root-mean-square roughness ( $R_q$ ) of 2.24 nm, the PF3-DTC-based one shows a significantly increased  $R_q$  of 6.56 nm and excessive phase separation due to the strong intermolecular self-aggregation behaviour, which inhibits the exciton dissociation, charge extraction, and charge transfer processes and thus leads to both lower  $J_{sc}$  and lower FF values in devices.

Moreover, compared with the PF2-DTC-based blend, the PF3-DTCO-based blend has the slightly increased  $R_q$  of 2.90 nm and a more uniform and distinct fibril texture. In accordance with the AFM results, the PM6:PF3-DTC blend shows excessive molecular aggregation and phase separation behaviour in the TEM study (Figure 3d), whereas PM6:PF3-DTCO blend presents more uniform phase separation and fibril texture, too. The improved molecular packing and blend morphology of the PM6:PF3-DTCO system are expected to improve the exciton dissociation, charge extraction, and transfer processes for achieving high  $J_{sc}$  and FF values in devices.

In conclusion, a NBG polymer acceptor PF3-DTCO based on an A–D–A-structured acceptor unit ITIC16 and a C–O-bridged donor unit DTCO was developed. The extension of conjugation of acceptor units from IDIC16 to ITIC16 results in the red-shifted absorption spectrum and improved absorption coefficient. Moreover, in addition to broadening the absorption spectrum due to the enhanced ICT effect, the introduction of C–O-bridged donor unit also improves the absorption coefficient and electron-mobility, as well as the molecular order and morphology of active layers. As a result, PF3-DTCO obtained a much higher PCE of 10.13% with a significantly increased  $J_{sc}$  of  $15.75 \text{ mA cm}^{-2}$  in all-PSCs compared with its original polymer acceptor PF2-DTC (PCE = 8.95% and  $J_{sc} = 13.82 \text{ mA cm}^{-2}$ ). Our work not only develops a novel high-performance polymer acceptor, but also provides a promising design strategy to construct D–A polymer acceptors with excellent optical absorption by systematic backbone engineering with extended conjugation and an enhanced ICT effect for efficient all-PSCs.

## Supporting Information

Supporting Information is available from the Wiley Online Library or from the author.

## Acknowledgements

Q.F. and R.M. contributed equally to this work. The authors thank the Swedish Research Council, the Swedish Research Council Formas, and the Wallenberg Foundation (2017.0186, 2016.0059) through the Wallenberg Academy Fellows program for financial support. L. Hou thanks the NSFC Project (61774077) for financial support. Support from Sino-Danish Centre for Education and Research is fully acknowledged.

## Conflict of Interest

The authors declare no conflict of interest.

## Keywords

all-polymer solar cells, carbon–oxygen bridging, optical absorption, polymer acceptors, power conversion efficiencies

Received: March 16, 2020

Revised: March 31, 2020

Published online:

- [1] a) Y. Lin, J. Wang, Z. Zhang, H. Bai, Y. Li, D. Zhu, X. Zhan, *Adv. Mater.* **2015**, *27*, 1170; b) J. Yuan, Y. Zhang, L. Zhou, G. Zhang, H.-L. Yip, T.-K. Lau, X. Lu, C. Zhu, H. Peng, P. A. Johnson, M. Leclerc, Y. Cao, J. Ulanski, Y. Li, Y. Zou, *Joule* **2019**, *3*, 1140.
- [2] a) Q. Fan, W. Su, M. Zhang, J. Wu, Y. Jiang, X. Guo, F. Liu, T. P. Russell, M. Zhang, Y. Li, *Sol. RRL* **2019**, *3*, 1900169; b) Q. Fan, W. Su, Y. Wang, B. Guo, Y. Jiang, X. Guo, F. Liu, T. P. Russell, M. Zhang, Y. Li, *Sci. China Chem.* **2018**, *61*, 531; c) Q. Fan, Y. Wang, M. Zhang, B. Wu, X. Guo, Y. Jiang, W. Li, B. Guo, C. Ye, W. Su, J. Fang, X. Ou, F. Liu, Z. Wei, T. C. Sum, T. P. Russell, Y. Li, *Adv. Mater.* **2018**, *30*, 1704546.
- [3] a) D. Baran, R. S. Shraf, D. A. Hanifi, M. Abdelsamie, N. Gasparini, J. A. Rohr, S. Holliday, A. Wadsworth, S. Lockett, M. Neophytou, C. J. Emmott, J. Nelson, C. J. Brabec, A. Amassian, A. Salleo, T. Kirchartz, J. R. Durrant, I. McCulloch, *Nat. Mater.* **2017**, *16*, 363; b) T. Liu, Z. Luo, Q. Fan, G. Zhang, L. Zhang, W. Gao, X. Guo, W. Ma, M. Zhang, C. Yang, Y. Li, H. Yan, *Energy Environ. Sci.* **2018**, *11*, 3275; c) W. Su, Q. Fan, X. Guo, X. Meng, Z. Bi, W. Ma, M. Zhang, Y. Li, *Nano Energy* **2017**, *38*, 510.
- [4] a) X. Du, T. Heumueller, W. Gruber, A. Classen, T. Unruh, N. Li, C. J. Brabec, *Joule* **2019**, *3*, 215; b) Q. Fan, Q. Zhu, Z. Xu, W. Su, J. Chen, J. Wu, X. Guo, W. Ma, M. Zhang, Y. Li, *Nano Energy* **2018**, *48*, 413.
- [5] Y. Cui, H. Yao, J. Zhang, T. Zhang, Y. Wang, L. Hong, K. Xian, B. Xu, S. Zhang, J. Peng, Z. Wei, F. Gao, J. Hou, *Nat. Commun.* **2019**, *10*, 2515.
- [6] a) T. Liu, Z. Luo, Y. Chen, T. Yang, Y. Xiao, G. Zhang, R. Ma, X. Lu, C. Zhan, M. Zhang, C. Yang, Y. Li, J. Yao, H. Yan, *Energy Environ. Sci.* **2019**, *12*, 2529; b) Z. Luo, R. Sun, C. Zhong, T. Liu, G. Zhang, Y. Zou, X. Jiao, J. Min, C. Yang, *Sci. China Chem.* **2020**, *63*, 361.
- [7] Y. Lin, B. Adilbekova, Y. Firdaus, E. Yengel, H. Faber, M. Sajjad, X. Zheng, E. Yarali, A. Seitkhan, O. M. Bakr, A. El-Labban, U. Schwingenschlogl, V. Tung, I. McCulloch, F. Laquai, T. D. Anthopoulos, *Adv. Mater.* **2019**, *31*, 1902965.
- [8] a) C. Sun, S. Qin, R. Wang, S. Chen, F. Pan, B. Qiu, Z. Shang, L. Meng, C. Zhang, M. Xiao, C. Yang, Y. Li, *J. Am. Chem. Soc.* **2020**, *142*, 1465; b) R. Ma, T. Liu, Z. Luo, Q. Guo, Y. Xiao, Y. Chen, X. Li, S. Luo, X. Lu, M. Zhang, Y. Li, H. Yan, *Sci. China Chem.* **2020**, *63*, 325.
- [9] X. Xu, K. Feng, Z. Bi, W. Ma, G. Zhang, Q. Peng, *Adv. Mater.* **2019**, *31*, 1901872.
- [10] L. Hong, H. Yao, Z. Wu, Y. Cui, T. Zhang, Y. Xu, R. Yu, Q. Liao, B. Gao, K. Xian, H. Y. Woo, Z. Ge, J. Hou, *Adv. Mater.* **2019**, *31*, 1903441.
- [11] P. Chao, H. Chen, Y. Zhu, H. Lai, D. Mo, N. Zheng, X. Chang, H. Meng, F. He, *Adv. Mater.* **2020**, *32*, 1907059.
- [12] S. Liu, J. Yuan, W. Deng, M. Luo, Y. Xie, Q. Liang, Y. Zou, Z. He, H. Wu, Y. Cao, *Nat. Photonics* **2020**, <https://doi.org/10.1038/s41566-019-0573-5>.
- [13] L. Meng, Y. Zhang, X. Wan, C. Li, X. Zhang, Y. Wang, X. Ke, Z. Xiao, L. Ding, R. Xia, H. L. Yip, Y. Cao, Y. Chen, *Science* **2018**, *361*, 1094.
- [14] Z. Zhou, W. Liu, G. Zhou, M. Zhang, D. Qian, J. Zhang, S. Chen, S. Xu, C. Yang, F. Gao, H. Zhu, F. Liu, X. Zhu, *Adv. Mater.* **2020**, *32*, 1906324.
- [15] L. Zhan, S. Li, T.-K. Lau, Y. Cui, X. Lu, M. Shi, C.-Z. Li, H. Li, J. Hou, H. Chen, *Energy Environ. Sci.* **2020**, *13*, 635.
- [16] J. Song, C. Li, L. Zhu, J. Guo, J. Xu, X. Zhang, K. Weng, K. Zhang, J. Min, X. Hao, Y. Zhang, F. Liu, Y. Sun, *Adv. Mater.* **2019**, *31*, 1905645.
- [17] Q. An, X. Ma, J. Gao, F. Zhang, *Sci. Bull.* **2019**, *64*, 504.
- [18] Z. Genene, W. Mammo, E. Wang, M. R. Andersson, *Adv. Mater.* **2019**, *31*, 1807275.
- [19] G. Wang, F. S. Melkonyan, A. Facchetti, T. J. Marks, *Angew. Chem., Int. Ed.* **2019**, *58*, 4129.
- [20] a) W. Su, Y. Meng, X. Guo, Q. Fan, M. Zhang, Y. Jiang, Z. Xu, Y. Dai, B. Xie, F. Liu, M. Zhang, T. P. Russell, Y. Li, *J. Mater. Chem. A* **2018**, *6*, 16403; b) W. Su, Q. Fan, X. Guo, B. Guo, W. Li, Y. Zhang, M. Zhang, Y. Li, *J. Mater. Chem. A* **2016**, *4*, 14752.
- [21] S. Chen, S. Jung, H. J. Cho, N. H. Kim, S. Jung, J. Xu, J. Oh, Y. Cho, H. Kim, B. Lee, Y. An, C. Zhang, M. Xiao, H. Ki, Z. Zhang, J. Y. Kim, Y. Li, H. Park, C. Yang, *Angew. Chem., Int. Ed.* **2018**, *57*, 13277.
- [22] D. Chen, J. Yao, L. Chen, J. Yin, R. Lv, B. Huang, S. Liu, Z. Zhang, C. Yang, Y. Chen, Y. Li, *Angew. Chem., Int. Ed.* **2018**, *57*, 4580.
- [23] H. Yao, F. Bai, H. Hu, L. Arunagiri, J. Zhang, Y. Chen, H. Yu, S. Chen, T. Liu, J. Y. L. Lai, Y. Zou, H. Ade, H. Yan, *ACS Energy Lett.* **2019**, *4*, 417.
- [24] R. Zhao, N. Wang, Y. Yu, J. Liu, *Chem. Mater.* **2020**, *32*, 1308.
- [25] Z. Zhang, Y. Yang, J. Yao, L. Xue, S. Chen, X. Li, W. Morrison, C. Yang, Y. Li, *Angew. Chem., Int. Ed.* **2017**, *56*, 13503.
- [26] H. Sun, Y. Tang, C. W. Koh, S. Ling, R. Wang, K. Yang, J. Yu, Y. Shi, Y. Wang, H. Y. Woo, X. Guo, *Adv. Mater.* **2019**, *31*, 1807220.
- [27] Y. Wu, S. Schneider, C. Walter, A. H. Chowdhury, B. Bahrami, H. C. Wu, Q. Qiao, M. F. Toney, Z. Bao, *J. Am. Chem. Soc.* **2020**, *142*, 392.
- [28] X. Liu, C. Zhang, C. Duan, M. Li, Z. Hu, J. Wang, F. Liu, N. Li, C. J. Brabec, R. A. J. Janssen, G. C. Bazan, F. Huang, Y. Cao, *J. Am. Chem. Soc.* **2018**, *140*, 8934.
- [29] N. B. Kolhe, D. K. Tran, H. Lee, D. Kuzuhara, N. Yoshimoto, T. Koganezawa, S. A. Jenekhe, *ACS Energy Lett.* **2019**, *4*, 1162.
- [30] Y. Guo, Y. Li, O. Awartani, H. Han, J. Zhao, H. Ade, H. Yan, D. Zhao, *Adv. Mater.* **2017**, *29*, 1700309.
- [31] B. Fan, W. Zhong, L. Ying, D. Zhang, M. Li, Y. Lin, R. Xia, F. Liu, H. L. Yip, N. Li, Y. Ma, C. J. Brabec, F. Huang, Y. Cao, *Nat. Commun.* **2019**, *10*, 4100.
- [32] X. Liu, Y. Zou, H. Q. Wang, L. Wang, J. Fang, C. Yang, *ACS Appl. Mater. Interfaces* **2018**, *10*, 38302.
- [33] Y. Xu, J. Yuan, S. Liang, J.-D. Chen, Y. Xia, B. W. Larson, Y. Wang, G. M. Su, Y. Zhang, C. Cui, M. Wang, H. Zhao, W. Ma, *ACS Energy Lett.* **2019**, *4*, 2277.
- [34] B. Lin, L. Zhang, H. Zhao, X. Xu, K. Zhou, S. Zhang, L. Gou, B. Fan, L. Zhang, H. Yan, X. Gu, L. Ying, F. Huang, Y. Cao, W. Ma, *Nano Energy* **2019**, *59*, 277.
- [35] Z. Li, L. Ying, P. Zhu, W. Zhong, N. Li, F. Liu, F. Huang, Y. Cao, *Energy Environ. Sci.* **2019**, *12*, 157.
- [36] L. Zhu, W. Zhong, C. Qiu, B. Lyu, Z. Zhou, M. Zhang, J. Song, J. Xu, J. Wang, J. Ali, W. Feng, Z. Shi, X. Gu, L. Ying, Y. Zhang, F. Liu, *Adv. Mater.* **2019**, *31*, 1902899.
- [37] Y. Meng, J. Wu, X. Guo, W. Su, L. Zhu, J. Fang, Z.-G. Zhang, F. Liu, M. Zhang, T. P. Russell, Y. Li, *Sci. China Chem.* **2019**, *62*, 845.
- [38] E. Zhou, M. Nakano, S. Izawa, J. Cong, I. Osaka, K. Takimiya, K. Tajima, *ACS Macro. Lett.* **2014**, *3*, 872.
- [39] H. Yan, Z. Chen, Y. Zheng, C. Newman, J. R. Quinn, F. Dotz, M. Kastler, A. Facchetti, *Nature* **2009**, *457*, 679.
- [40] Z. Li, X. Xu, W. Zhang, X. Meng, W. Ma, A. Yartsev, O. Inganäs, M. R. Andersson, R. A. Janssen, E. Wang, *J. Am. Chem. Soc.* **2016**, *138*, 10935.
- [41] T. Kim, J. H. Kim, T. E. Kang, C. Lee, H. Kang, M. Shin, C. Wang, B. Ma, U. Jeong, T. S. Kim, B. J. Kim, *Nat. Commun.* **2015**, *6*, 8547.
- [42] H. Bente, T. Nishida, D. Mori, H. Xu, H. Ohkita, S. Ito, *Energy Environ. Sci.* **2016**, *9*, 135.
- [43] N. Zhou, A. S. Dudnik, T. I. Li, E. F. Manley, T. J. Aldrich, P. Guo, H. C. Liao, Z. Chen, L. X. Chen, R. P. Chang, A. Facchetti, C. M. Olvera, T. J. Marks, *J. Am. Chem. Soc.* **2016**, *138*, 1240.
- [44] J. Wu, Y. Meng, X. Guo, L. Zhu, F. Liu, M. Zhang, *J. Mater. Chem. A* **2019**, *7*, 16190.

- [45] Q. Fan, W. Su, S. Chen, W. Kim, X. Chen, B. Lee, T. Liu, U. A. Méndez-Romero, R. Ma, T. Yang, W. Zhuang, Y. Li, Y. Li, T.-S. Kim, L. Hou, C. Yang, H. Yan, D. Yu, E. Wang, *Joule* **2020**, *4*, 658.
- [46] a) J. Song, M. Zhang, M. Yuan, Y. Qian, Y. Sun, F. Liu, *Small Methods* **2018**, *2*, 1700229; b) Q. Fan, T. Liu, M. Zhang, W. Su, U. A. Méndez-Romero, T. Yang, X. Geng, L. Hou, D. Yu, F. Liu, H. Yan, E. Wang, *Small Methods* **2020**, *4*, 1900766.
- [47] P. W. M. Blom, V. D. Mihailetschi, L. J. A. Koster, D. E. Markov, *Adv. Mater.* **2007**, *19*, 1551.